





## Article

# Frequency Splitting Elimination and Cross-Coupling Rejection of Wireless Power Transfer to Multiple Dynamic Receivers

Narayanamoorthi R. <sup>1</sup> , Vimala Juliet <sup>2</sup>, Sanjeevikumar Padmanaban <sup>3</sup> ,  
Lucian Mihet-Popa <sup>4,\*</sup>  and Bharatiraja C. <sup>1</sup> 

<sup>1</sup> Department of Electrical and Electronics Engineering, SRM University, Chennai 603 203, India; narayanamoorthi.r@gmail.com (N.R.); bharatiraja@gmail.com (B.C.)

<sup>2</sup> Department of Electronics and Instrumentation Engineering, SRM University, Chennai 603 203, India; vimlala@yahoo.co.in

<sup>3</sup> Department of Energy Technology, Aalborg University, 6700 Esbjerg, Denmark; sanjeevi\_12@yahoo.co.in

<sup>4</sup> Faculty of Engineering, Østfold University College, Kobblerlagerstredet 5, 1671 Kråkerøy-Fredrikstad, Norway

\* Correspondence: lucian.mihet@hiiof.no; Tel.: +47-922-713-53

Received: 6 December 2017; Accepted: 16 January 2018; Published: 26 January 2018

**Abstract:** Simultaneous power transfer to multiple receiver (Rx) system is one of the key advantages of wireless power transfer (WPT) system using magnetic resonance. However, determining the optimal condition to uniformly transfer the power to a selected Rx at high efficiency is the challenging task under the dynamic environment. The cross-coupling and frequency splitting are the dominant issues present in the multiple Rx dynamic WPT system. The existing analysis is performed by considering any one issue present in the system; on the other hand, the cross coupling and frequency splitting issues are interrelated in dynamic Rx's, which requires a comprehensive design strategy by considering both the problems. This paper proposes an optimal design of multiple Rx WPT system, which can eliminate cross coupling, frequency splitting issues and increase the power transfer efficiency (PTE) of selected Rx. The cross-coupling rejection, uniform power transfer is performed by adding an additional relay coil and independent resonance frequency tuning with capacitive compensation to each Rx unit. The frequency splitting phenomena are eliminated using non-identical transmitter (Tx) and Rx coil structure which can maintain the coupling between the coil under the critical coupling limit. The mathematical analysis of the compensation capacitance calculation and optimal Tx coil size identification is performed for the four Rx WPT system. Finite element analysis and experimental investigation are carried out for the proposed design in static and dynamic conditions.

**Keywords:** wireless power transfer; frequency splitting; cross-coupling; multiple receivers; magnetic resonance

## 1. Introduction

Recent progress in the magnetic resonant based wireless power transfer (MRWPT) system has stimulated its usage in wide applications such as electric vehicles, consumer appliances, and wireless sensor networks [1–3]. Also, MRWPT technology could be the best choice for small power wearable or implanted healthcare devices, such as blood glucose monitors, hearing aids, electrocardiogram, micropumps, pacemakers and insulin pumps [4,5]. Similarly, with the advent of microelectronics and semiconductor technology the size of these devices is shrinking drastically, which makes the device portable or even implantable [6,7]. In the meantime, the number of personal electronic devices used by a person is increasing day by day, which needs to be charged efficiently from a single power source [8].

MRWPT system turns to be the suitable choice to simultaneously power multiple devices by a single source [9]. However, the simultaneous power transfer to multiple devices presents to be more challenging regarding coil optimization and uniform power distribution. Moreover, under dynamic conditions, the power delivered to the receiving units is reduced due to the presence of cross coupling and frequency splitting issues [10,11]. In [12], single Tx and multiple Rx system are investigated for the static load conditions with fixed operating frequency. However, in the practical scenario, the power rating and operating frequency of the devices cannot be maintained at the same level. Likewise, the uniform power distribution to multiple loads is challenging to attain using a single Tx coil with fixed operating frequency. On the other hand, the multiple Tx's are examined to increase the power delivery capacity to multiple loads [13,14]. Even though, multiple Tx's can provide stable power to all the loads, the increase in the number of Tx will not be the preferred solution for small-scale power applications [15].

To increase the power transfer efficiency (PTE), relay coils are normally employed in the single Tx and Rx WPT system [16,17]. These relay coils can improve the quality factor of the Tx, Rx and load coils, thereby improvement in the PTE of WPT system. However, the addition of relay coils in multiple Rx system requires an optimal design of the coil structure and coupling between the Tx and Rx coils [18]. Meanwhile, the coil optimization and addition of ferrite core materials to improve the magnetic coupling are studied for high power applications [19,20]. Nevertheless, in case of lower power devices addition of ferrite core material is restricted and requires an alternative way for power transfer technique.

The three-dimensional Tx coil structure is investigated for the maximum power transfer to single dynamic Rx irrespective of the orientation [21,22]. However, the uniform power distribution to multiple Rx with three-dimensional structure is difficult to control and requires additional control circuitry at the Tx coil. Time division multiplexing based power transfer to multiple Rx approach was examined to uniformly transfer the power to individual loads [23]. In this approach, the Rx coils are designed with different resonant frequency, and the Tx frequency is varied to match with the Rx coil frequency. However, in practical scenarios more than one Rx's might be designed with a same resonant frequency which leads to cross-coupling between the Rx coils [24,25].

To eliminate the cross coupling between the coils, compensation circuits are employed for the multiple Rx system [26]. The capacitive compensation at the Rx coil was studied for static load conditions and proved to be an effective way to filter the non-resonant magnetic field from the adjacent Rx coils [27]. The capacitive compensation also takes less space and turns to be effective in low power device fabrication. However, under the dynamic condition, the continuous variation in the Rx position leads to the frequency splitting in the Rx coil power with cross-coupling among the Rx unit [28].

Frequency splitting is the deviation in the resonant frequency of the system due to overcoupling between the Tx and Rx coils. In [29], the auto-tuning of the impedance matching circuit has been discussed to minimize the effects of frequency splitting for the single Tx and Rx system. In case of multiple Rx system which is operated at different resonant frequency employing the impedance matching circuit increases the design complexity and requires a wide range of capacitance and inductive elements. Therefore, to minimize the effects of frequency splitting with simple control approach a non-identical resonant coil structure was studied for different distance in single Tx and Rx system [30,31]. However, in case of lower power multiple, Rx WPT system the size of the Rx coils is restricted which requires the optimal design of non-identical Tx and Rx coil by considering the Rx coil size constraints.

Based on the above discussion, it is observed that for the multiple Rx WPT system under dynamic environment, the cross-coupling, frequency splitting, uniform power distribution to all the Rx with improved PTE are a major challenge. It is also noted that all these issues are interrelated to each other and requires an optimal design in multiple Rx's by considering all the challenges. This paper proposes a selective resonance WPT to multiple Rx's using Tx frequency tuning circuit. Further to improve the PTE, an additional relay coil is added to each Rx's which can reduce the effect of load port resistance

and improve the quality factor. The cross-coupling effect is minimized by determining the optimal value of the compensation reactance and connecting across each load coil. Frequency splitting under the over-coupling condition is eliminated by choosing a non-identical resonant Tx coil structure at the minimum possible coupling distance.

The paper is organized as in Section 2 the basic structure of the multiple Rx's WPT system at different configurations is presented. In Section 3, the performance improvement and design strategies of the proposed method is discussed. The validation of the proposed method using finite element simulation and experimental measurements are presented in Sections 4 and 5 respectively.

## 2. Dynamic Multiple Receiver

The different possible combinations of multiple Rx's with single Tx WPT system schematic model is shown in Figure 1. The Tx is supplied using high frequency inverter/power amplifier and the Rx coils are connected to the load. Both the Tx and Rx coils are configured in series-series topology of resonant capacitor and inductor. Parasitic resistance of all the elements are combined with the source and load port resistance of the respective coil. Figure 1a represents the four Rx's are in a static condition with same resonant frequency and placed at a fixed distance between Tx and Rx [32]. In this case, the cross-coupling among the Rx's will be a major concern. In Figure 1b the multiple Rx's designed with dissimilar resonant frequency and placed at a different distance is illustrated. Similarly, the Figure 1c shows the identical coil with same resonant frequency placed at a different distance between the Tx and Rx [33]. The main issue in identical resonant frequency configuration is the cross-coupling effect among the Rx's will be more and its minimum in the non-identical resonant frequency configuration, however, the bandwidth of the frequency among the Rx must be large. The third configuration which represents the dynamic condition of the Rx's will produce both cross coupling and frequency splitting whenever the coupling is increased more than the critical coupling point.

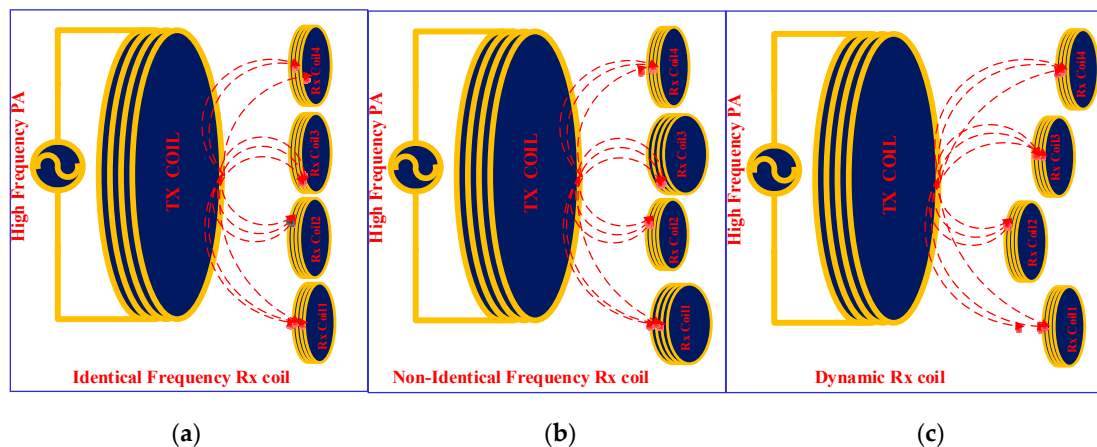


**Figure 1.** Possible dynamic receiver configuration. (a) Identical Rx's; (b) Nonidentical Rx's; (c) Dynamic Rx's.

## 3. Performance Improvement of Multiple Receiver WPT

To improve the performance of the multiple Rx's systems with uniform power distribution, cross-coupling reduction, and frequency splitting elimination in the multiple Rx WPT system is discussed in this section.

### 3.1. Power Transfer Efficiency Improvement

The PTE of the MRWPT system primarily influenced by the coupling, quality factor of the Tx and Rx coil. Quality factor of the coil reduces due to the increase in the source and load port resistance of the circuit, which can be minimized by adding a relay coil to the circuit. The three coil WPT circuit gives a better power delivered to the load and PTE as compared with the four coil WPT circuit [34].

However, for the selective power distribution using time division multiplexing requires to tune the Tx coil frequency which makes difficult to add a relay coil at the transmitter section. In this work the additional relay coil is used at the Rx side and called as the load coil. The equivalent circuit of three coil MRWPT system is shown in Figure 2, consist of Tx coil, Rx coil and load coil.  $R_1$ ,  $R_2$ ,  $R_L$ ,  $L_1$ ,  $L_2$ ,  $L_3$ ,  $C_1$ ,  $C_2$ ,  $C_3$ ,  $Q_T$ ,  $Q_R$  and  $Q_L$  are the Tx, Rx and load coil resistance, self-inductance, capacitance, quality factor respectively.

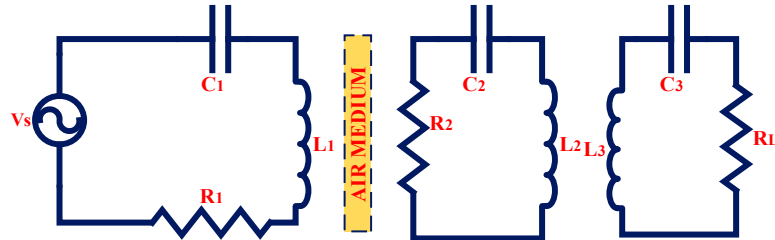


**Figure 2.** Equivalent circuit of three coil magnetic resonant based wireless power transfer (MRWPT) system.

The equivalent network model of the circuit is formulated by applying KVL to each coil

$$\begin{bmatrix} V_T \\ 0 \\ 0 \end{bmatrix} = \begin{bmatrix} Z_{11} & Z_{12} & Z_{13} \\ Z_{21} & Z_{22} & Z_{23} \\ Z_{31} & Z_{32} & Z_{33} \end{bmatrix} \begin{bmatrix} I_1 \\ I_2 \\ I_3 \end{bmatrix} \quad (1)$$

where  $I_1$ ,  $I_2$  and  $I_3$  are the current in Tx, Rx and load coil respectively. The self-impedance ( $Z_{ij}, i = j$ ), mutual impedance ( $Z_{ij}, i \neq j$ ) and coupling coefficient  $k_{ij}$  of the system can be expressed as

$$Z_{ij} = Z_{ji} = R_i + j\omega L_i + \frac{1}{j\omega C_i}; \text{ for } i = j$$

$$Z_{ij} = Z_{ji} = j\omega M_{ij} = j\omega K_{ij} \sqrt{L_i L_j}; \text{ for } i \neq j \quad (2)$$

$$k_{ij} = \frac{M_{ij}}{\sqrt{L_i L_j}} \quad (3)$$

The RMS value of input, output power and efficiency of the three coil MRWPT system as

$$P_T = \frac{1}{2} V_T I_1 \quad (4)$$

$$P_{OUT} = \frac{1}{2} I_3^2 R_L \quad (5)$$

After solving the Equations (1) and (5) using (2), the efficiency of the system is given as

$$\eta_{3coil} = \frac{k_{12}^2 k_{23}^2 Q_T Q_R^2 Q_L}{(1 + k_{12}^2 Q_T Q_R + k_{23}^2 Q_R Q_L)(1 + k_{23}^2 Q_R Q_L)} \quad (6)$$

The total amount of power delivered to the load coil can be found by multiplying efficiency with source power

$$P_L = \frac{V_T^2 k_{12}^2 k_{23}^2 Q_T Q_R^2 Q_L}{2 R_1 (1 + k_{12}^2 Q_T Q_R + k_{23}^2 Q_R Q_L)^2} \quad (7)$$

The variation of system efficiency and PDL concerning  $k_{23}$  and  $d_{23}$  are shown in Figure 3a,b. It can be seen that by choosing an optimal values of  $k_{12}$  and  $k_{23}$  the overall system efficiency and PDL can be maximized.



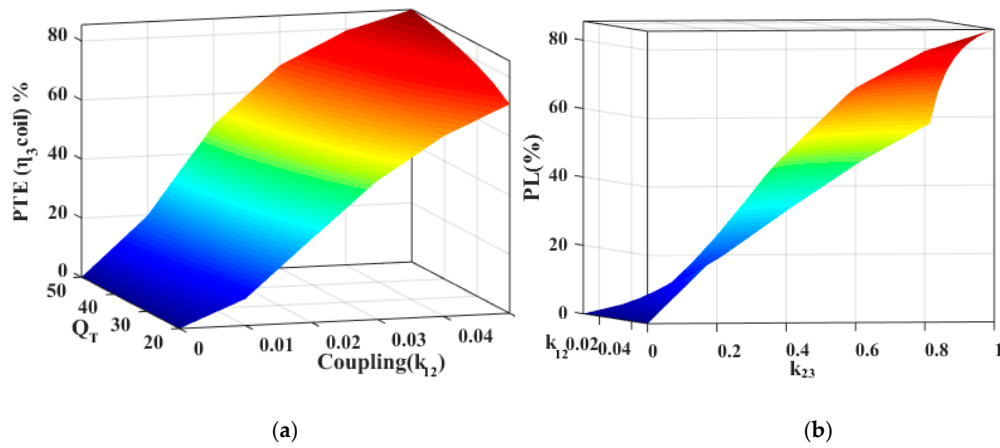


**Figure 3.** Three coil circuit response (a) Power transfer efficiency; (b) Power delivered to load.

### 3.2. Selective MRWPT System

The equivalent circuit of multiple receiver selective MRWPT system is illustrated in Figure 4. For the analysis, the system is chosen with four Rx coils, four load coils, and single Tx coil. The Tx, Rx, and load coil parameters are denoted by the subscript of  $T$ ,  $R_i$ , and  $L_i$  ( $i = 1, 2, 3, 4$ ) respectively. The PTE of the particular system can be maximized when the operating frequency is same as the Tx, Rx and load coil resonant frequency. Using this principle, the selective power transfer to multiple receivers can be achieved by tuning the transmitter side capacitance to match the operating frequency to be same as the Rx and Load resonant frequency. The resonant frequency of the receiver loops  $f_{r1}$ ,  $f_{r2}$ ,  $f_{r3}$  and  $f_{r4}$  are calculated as

$$\begin{aligned} f_{r1} &= \frac{1}{2\pi\sqrt{L_{R1}C_{R1}}} = \frac{1}{2\pi\sqrt{L_{L1}C_{L1}}}; f_{r2} = \frac{1}{2\pi\sqrt{L_{R2}C_{R2}}} = \frac{1}{2\pi\sqrt{L_{L2}C_{L2}}} \\ f_{r3} &= \frac{1}{2\pi\sqrt{L_{R3}C_{R3}}} = \frac{1}{2\pi\sqrt{L_{L3}C_{L3}}}; f_{r4} = \frac{1}{2\pi\sqrt{L_{R4}C_{R4}}} = \frac{1}{2\pi\sqrt{L_{L4}C_{L4}}} \end{aligned} \quad (8)$$

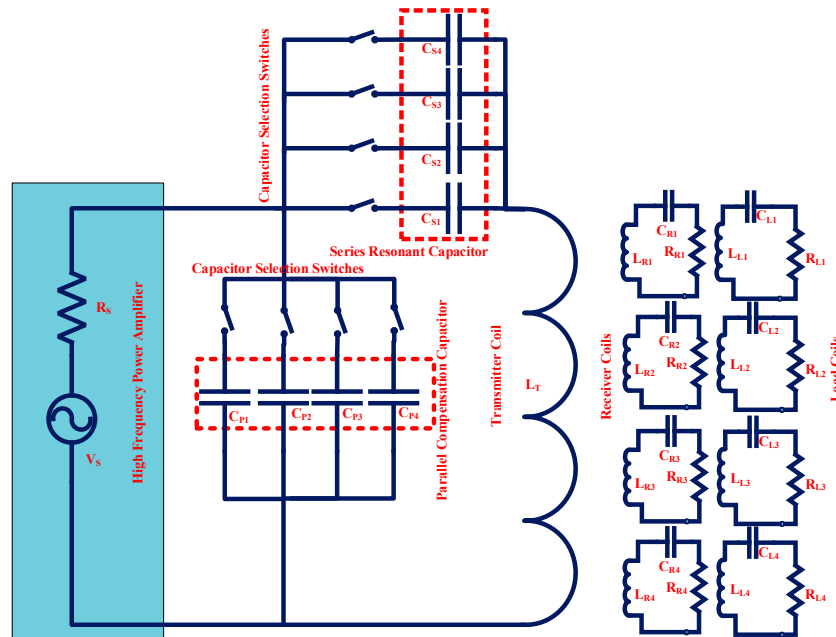


**Figure 4.** Equivalent circuit of Selective MRWPT system.

Even though the receiver devices are designed with different resonant frequencies and selected to transfer the power uniformly to individual load there exist a cross-coupling between Tx and unselected Rx coils. For the reason that of the non-resonant coupling effect, there exists an inter cross-coupling among the Rx coils. As the number of coils with different resonant frequency is increasing the cross-coupling also increases which reduces the PTE of the selected link. The simulated response of the selective MRWPT system is presented in Figure 5. The four Rx and load coils are designed with the resonant frequency of 1.0 MHz, 1.50 MHz, 2.0 MHz, 3.0 MHz with the circuit parameters mentioned in Table 1. Initially, the Rx1 coil is selected by tuning the Tx coil to 1 MHz, and the response of the system is shown in Figure 5a, the peak magnitude occurs at 1 MHz along with that the unselected load coils magnitude are in the range of  $-18$  dB at their respective resonant frequency. Likewise, the resonant frequency of the Tx coils is tuned to 1.5 MHz, 2 MHz, and 3 MHz to match with the Rx2 to Rx4 resonant frequency as shown in Figure 5b–d. Since the passband frequency of the system has much overlapping with other resonant frequency there exist a cross-coupling effect in all the link. The effects of cross-coupling need to be minimized to transfer the power uniformly to selected load at high efficiency.

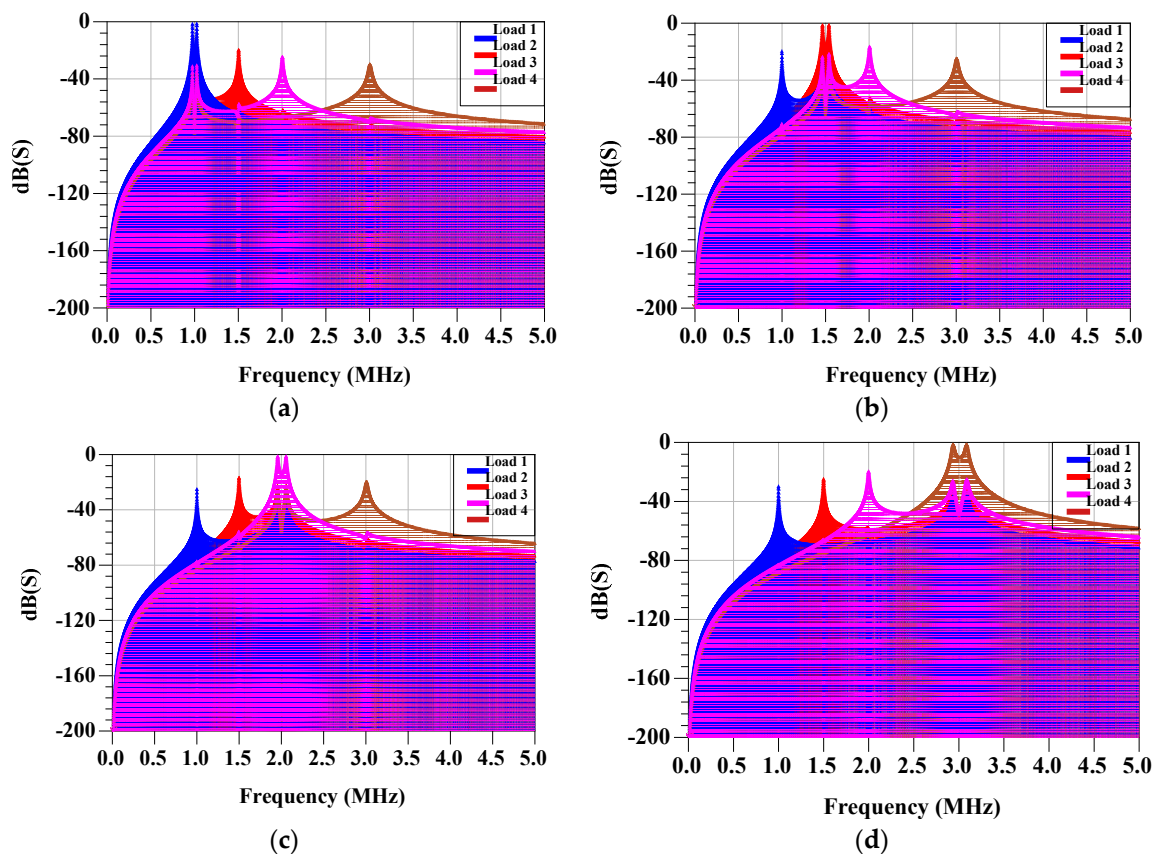


**Figure 5.** S Parameter dB of the system without compensation (a) dB(S) when Rx1-on; (b) dB(S) when Rx2-on; (c) dB(S) when Rx3-on; (d) dB(S) when Rx4-on.

**Table 1.** Circuit design parameters.

Parameters	Tx	Rx1/Load1	Rx2/Load2	Rx3/Load3	Rx4/Load4
Frequency (MHz)	-	1.0	1.5	2.0	3.0
Inductance ( $\mu$ H)	112.58	25.33	11.248	6.333	2.814
Capacitance (nF)	-	10	10	10	10
Resistance ( $\Omega$ )	50.5	0.5/50.5	0.5/50.5	0.5/50.5	0.5/50.5

### 3.3. Cross-Coupling Rejection

Even though all the Rx coils are designed with different resonant frequency in selective MRWPT system, the cross coupling between the coil is unavoidable. Also under the dynamic environment, the multiple Rx coils position will keep on change, and there exists a cross-coupling between the coils. The wide range selection of different resonant frequency between the receiver is limited in some applications like medical implants and tiny electronics, which leads to resonant frequency overlapping between the Rx coils. Moreover, when the separation among the Tx and Rx coils are reducing below the critical value, frequency splitting will be present in the system which leads to the variation in the resonant frequency and increases the cross coupling between the coil. In order to overcome the effects of cross coupling and increase the PTE of the selective MRWPT system, the compensation is required at each load coil.

The optimal value of the compensation reactance is calculated by applying KVL to Figure 6.

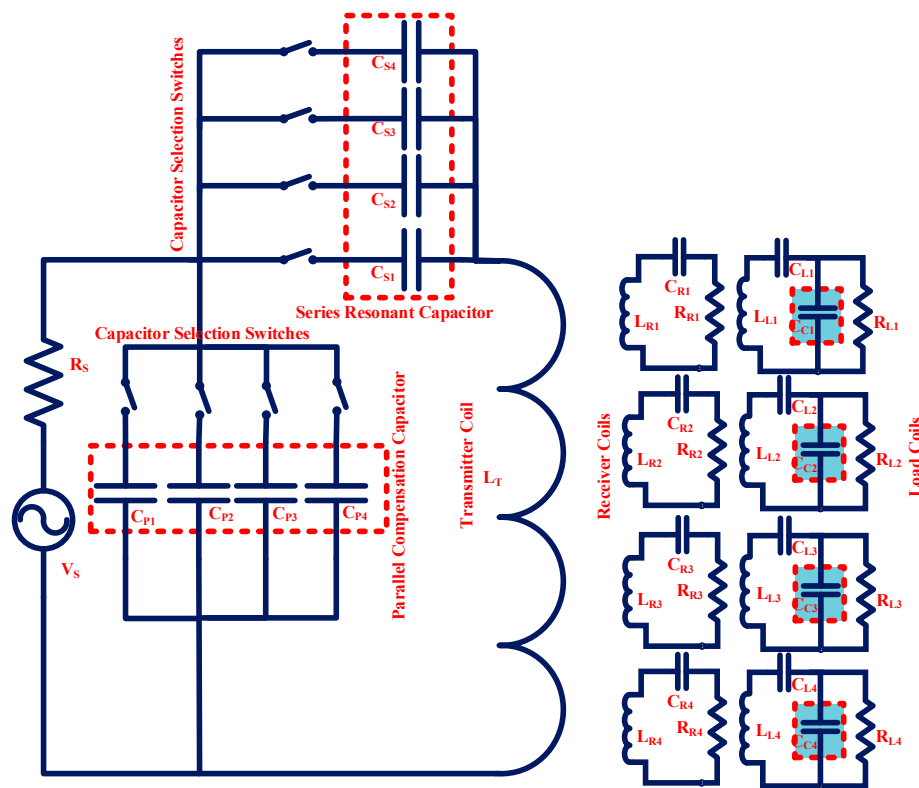


Figure 6. Equivalent circuit of Selective MRWPT system with Compensation.

$$\begin{bmatrix} V_T \\ 0 \\ 0 \\ 0 \\ 0 \\ 0 \\ 0 \\ 0 \\ 0 \end{bmatrix} = \begin{bmatrix} Z_{TT} & Z_{TR1} & Z_{TR2} & Z_{TR3} & Z_{TR4} & Z_{TL1} & Z_{TL2} & Z_{TL3} & Z_{TL4} \\ Z_{R1T} & Z_{R1R1} & Z_{R1R2} & Z_{R1R3} & Z_{R1R4} & Z_{R1L1} & Z_{R1L2} & Z_{R1L3} & Z_{R1L4} \\ Z_{R2T} & Z_{R2R1} & Z_{R2R2} & Z_{R2R3} & Z_{R2R4} & Z_{R2L1} & Z_{R2L2} & Z_{R2L3} & Z_{R2L4} \\ Z_{R3T} & Z_{R3R1} & Z_{R3R2} & Z_{R3R3} & Z_{R3R4} & Z_{R3L1} & Z_{R3L2} & Z_{R3L3} & Z_{R3L4} \\ Z_{R4T} & Z_{R4R1} & Z_{R4R2} & Z_{R4R3} & Z_{R4R4} & Z_{R4L1} & Z_{R4L2} & Z_{R4L3} & Z_{R4L4} \\ Z_{L1T} & Z_{L1R1} & Z_{L1R2} & Z_{L1R3} & Z_{L1R4} & Z_{L1L1} & Z_{L1L2} & Z_{L1L3} & Z_{L1L4} \\ Z_{L2T} & Z_{L2R1} & Z_{L2R2} & Z_{L2R3} & Z_{L2R4} & Z_{L2L1} & Z_{L2L2} & Z_{L2L3} & Z_{L2L4} \\ Z_{L3T} & Z_{L3R1} & Z_{L3R2} & Z_{L3R3} & Z_{L3R4} & Z_{L3L1} & Z_{L3L2} & Z_{L3L3} & Z_{L3L4} \\ Z_{L4T} & Z_{L4R1} & Z_{L4R2} & Z_{L4R3} & Z_{L4R4} & Z_{L4L1} & Z_{L4L2} & Z_{L4L3} & Z_{L4L4} \end{bmatrix} \begin{bmatrix} I_T \\ I_{R1} \\ I_{R2} \\ I_{R3} \\ I_{R4} \\ I_{L1} \\ I_{L2} \\ I_{L3} \\ I_{L4} \end{bmatrix} \quad (9)$$

Since the Tx coil coupling with load coil is negligible as compared with Tx and Rx, the mutual inductance  $M_{TL1}$ ,  $M_{TL2}$ ,  $M_{TL3}$ ,  $M_{TL4}$ ,  $M_{L1T}$ ,  $M_{L2T}$ ,  $M_{L3T}$  and  $M_{L4T}$  could be assumed as zero. Under the resonance condition the reactive impedance of the circuit is cancelled and only the resistance, of the coil is present. Resolving (8) the obtained value of Rx coil and load coil current is

$$I_i = -\sum_{k=1, i \neq k}^4 \frac{j\omega_i M_{Ti} M_{ik} I_T}{R_i + R_k + R_{Li}}; \quad i = R_k, L_k \quad (10)$$

Using (10) the input port impedance can be calculated by substituting in the first row of (9)

$$Z_{in} = R_T + \sum_{k=1}^4 \frac{\omega^2 M_{Ti}^2}{R_T + R_{Li}}; \quad i = R_k, L_k \quad (11)$$

From (9) and (10) we can observe that the cross-coupling between the receiver loop coil is not many negligible variations will occur in the input current and input port impedance which leads to a reduction in the overall power transfer efficiency. The optimal value of the load reactance is calculated from (10) and (11)

$$X_{L1} = -\sum_{k=R1, \dots, R4} \frac{\omega_1 M_{TR1} M_{R1k} (R_2 + R_{L2})}{M_{Tk} (R_k + R_{L2})} \quad (12)$$

$$X_{L2} = -\sum_{k=R1, \dots, R4} \frac{\omega_2 M_{TR2} M_{R2k} (R_4 + R_{L4})}{M_{Tk} (R_k + R_{L4})} \quad (13)$$

$$X_{L3} = -\sum_{k=R1, \dots, R4} \frac{\omega_3 M_{TR3} M_{R3k} (R_6 + R_{L6})}{M_{Tk} (R_k + R_{L6})} \quad (14)$$

$$X_{L4} = -\sum_{k=R1, \dots, R4} \frac{\omega_4 M_{TR4} M_{R4k} (R_6 + R_{L6})}{M_{Tk} (R_k + R_{L6})} \quad (15)$$

where  $X_{L1}$ ,  $X_{L2}$ ,  $X_{L3}$  and  $X_{L4}$  are the additional inductance added to the load coils to compensate the cross coupling. Optimal value of load reactance be subject to the mutual inductance between the coils, load resistance and coil resistances and the equivalent circuit of the selective MRWPT system with compensation is shown in Figure 6. In practical implementations the maximum possible value of the mutual inductance between the coils are calculated and using discrete capacitor tuning the optimal load reactance can be achieved. The simulated response of the selective MRWPT system with cross coupling compensation is illustrated in Figure 7. Figure 7a display the dB value of S parameter when the Tx is operated at 1 MHz, it's observed from the graph that the unselected link has less cross coupling effect in the order of  $-50$  dB. Similarly, when the Tx is operated at 1.5 MHz, 2 MHz and 3 MHz resonant frequency the S parameter responses are shown in Figure 7b–d. In all the cases the unselected load S parameter value is less than  $-50$  dB, which indicates the much reduction in the cross coupling effect. The calculated capacitance values and circuit parameters are shown in Table 2. However, the effect of frequency splitting needs to be considered in the design whenever the coils are used in dynamic environment. All the simulations are performed at the constant coupling coefficient value of 0.1 between the Tx and Rx coil.

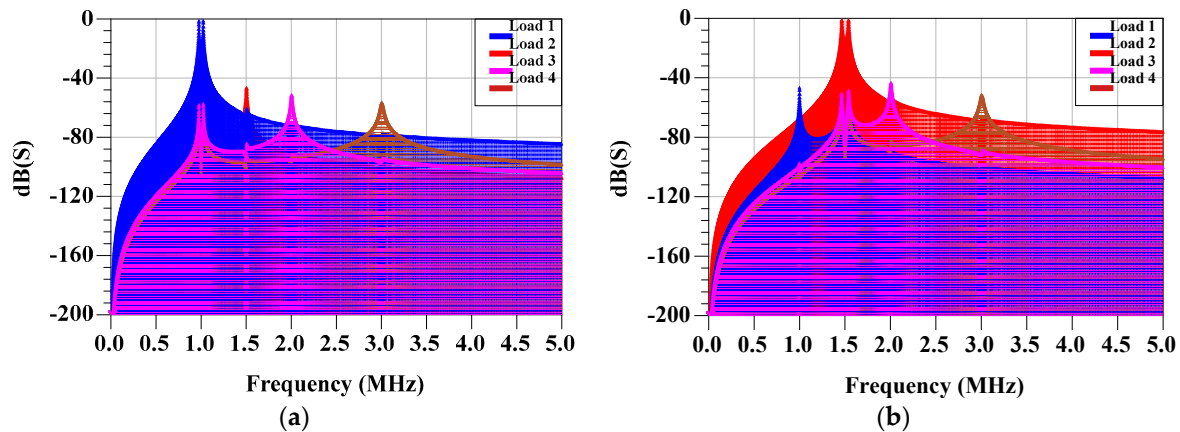
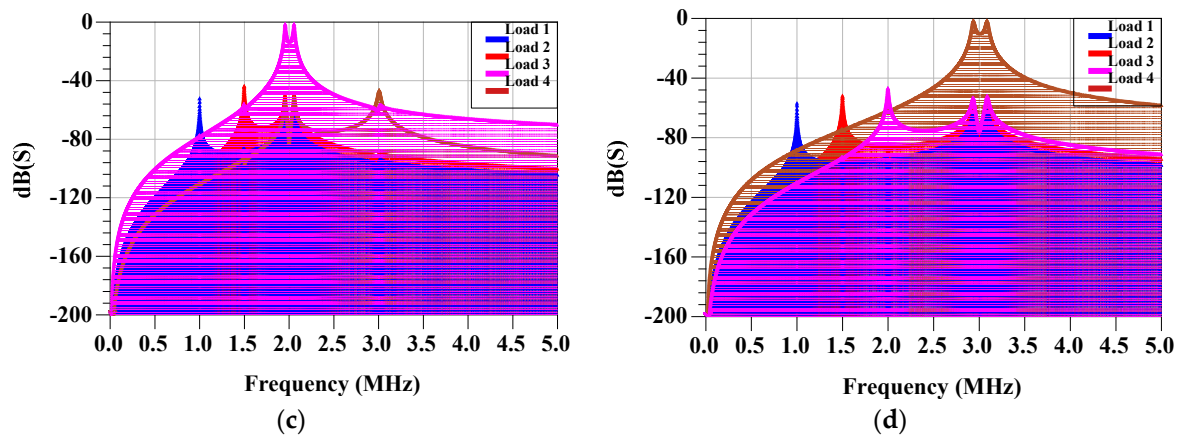


Figure 7. Cont.



**Figure 7.** dB of the coil with cross-coupling compensation (a) dB(S) when Rx1-on; (b) dB(S) when Rx2-on (c) dB(S) when Rx3-on; (d) dB(S) when Rx4-on.

### 3.4. Frequency Splitting Elimination

In the dynamic environment, the movement of the Rx devices causes the changes in the magnetic over the coupling and leads to frequency splitting. It degrades the system efficiency also the fluctuation in the output power of the receiver loop, which can be avoided by maintaining the mutual inductance of Tx and Rx section is almost constant irrespective of the coil separation. The non-identical coil structures can be used to eliminate the frequency splitting by keeping the mutual inductance to be constant irrespective of the distance variation. However, the PTE of the system depends on the coupling between the coil, many reductions in the mutual inductance can minimize the system efficiency. To determine the optimal coil radius, considering the Rx and Tx coils are having the radius of  $r_{R1}$ ,  $r_{R2}$ ,  $r_{R3}$ ,  $r_{R4}$ ,  $r_T$  and the separation distance of  $d_i$ . The mutual inductance  $M$  can be derived as [35]

$$M = \mu_0 \frac{\sqrt{r_T r_i}}{g} \left[ (2 - g^2) K(g^2) - 2E(g^2) \right] \text{ where } i = R_x, L_x \quad (16)$$

$$g^2 = \frac{4r_T r_i}{d_i^2 + (r_T + r_i)^2} \quad (17)$$

where  $E(*)$  and  $K(*)$  are the second and first order complete elliptic integrals. As the separation between the Tx and Rx approaches to zero, the term  $g^2$  becomes one when the radius of the coils are same. At  $g^2 = 1$ , the first order and, second order elliptic integrals become infinite and one respectively which makes rapid increase in the mutual inductance when the distance reduces. In order to overcome the above constraint  $g^2$  must be kept less than unity also without affecting the coupling and system efficiency for large separation gap between Tx and Rx unit. A different set of mutual inductance are calculated for various  $d_T$  and  $d_{R1}$ ,  $d_{R2}$ ,  $d_{R3}$ ,  $d_{R4}$  as illustrated in Figure 8. As the diameter of the Tx coil is increased the mutual inductance values are reduced for the small gap and changes very less for the larger air gap separation. However, when the diameter of the Tx coil is less the variation in the mutual inductance is drastic over the distance. From Figure 8 it's observed that the changes in the mutual inductance for the Tx coil diameter of 12.5 c.m is from 0.67 to 0.59 for the distance 2 c.m to 10 c.m and almost constant from 2 c.m to 8 c.m of distance between the coil. Further increase in the Tx coil diameter of 14.5 c.m, 15.5 c.m result in reduction of the mutual inductance value which can reduce the PTE and the comparison of mutual inductance for selected diameter is presented in Table 2. Hence an optimal value of 12.5 c.m Tx coil diameter is selected for the design to eliminate the frequency splitting by considering the PTE. However, the size of the Tx coil will change depending on the number of Rx, distance, diameter of Rx and number of turns.

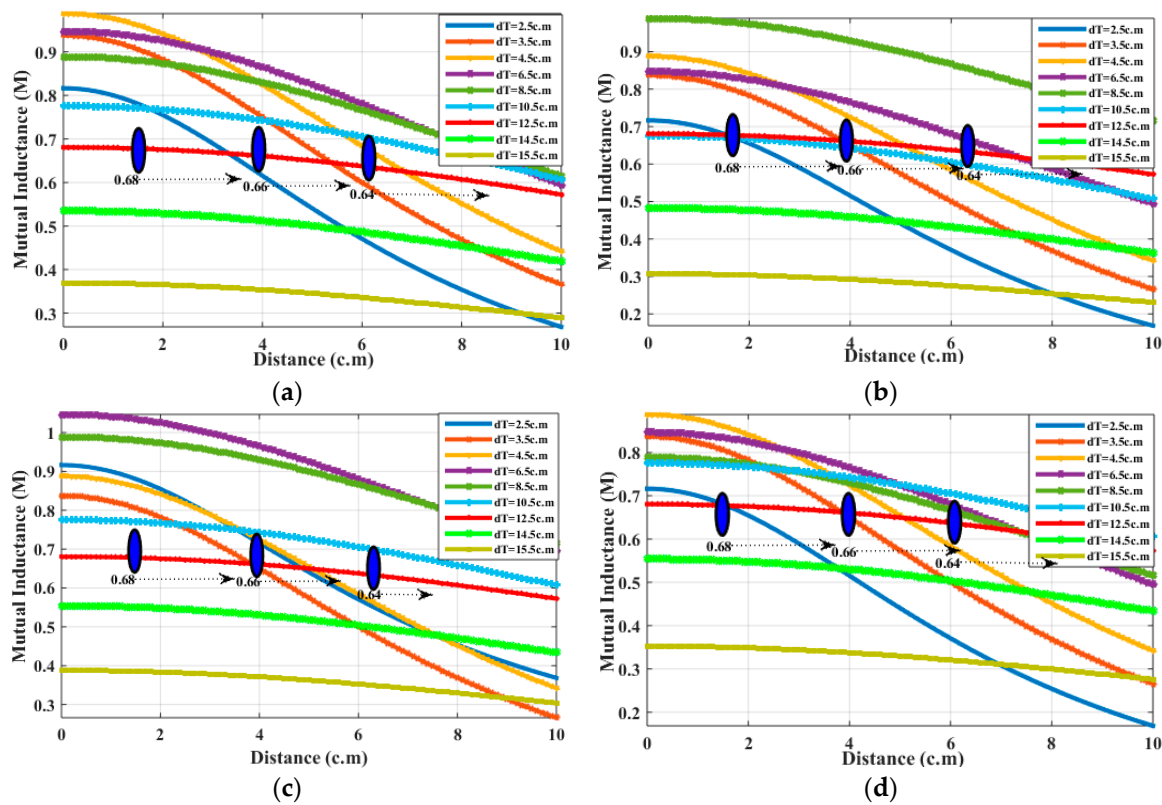


**Figure 8.** Mutual inductance values for different transmitter diameter (a)  $d_{R1} = d_{R2} = d_{R3} = d_{R4} = 4$  c.m.; (b)  $d_{R1} = 4.5$  c.m.,  $d_{R2} = 4$  c.m.,  $d_{R3} = 3.5$  c.m.,  $d_{R4} = 3$  c.m.; (c)  $d_{R1} = 4.5$  c.m.,  $d_{R2} = 4.5$  c.m.,  $d_{R3} = 3$  c.m.,  $d_{R4} = 3$  c.m.; (d)  $d_{R1} = 4$  c.m.,  $d_{R2} = 4$  c.m.,  $d_{R3} = 3.5$  c.m.,  $d_{R4} = 3$  c.m.

**Table 2.** Mutual inductance at different Tx and Rx coil diameters.

Distance (c.m.)	$d_{R1} = 4.0$ c.m., $d_{R2} = 4.0$ c.m., $d_{R3} = 4.0$ c.m., $d_{R4} = 4.0$ c.m.				$d_{R1} = 4.5$ c.m., $d_{R2} = 4.0$ c.m., $d_{R3} = 3.5$ c.m., $d_{R4} = 3.0$ c.m.				$d_{R1} = 4.5$ c.m., $d_{R2} = 4.5$ c.m., $d_{R3} = 3.0$ c.m., $d_{R4} = 3.0$ c.m.				$d_{R1} = 4.0$ c.m., $d_{R2} = 4.0$ c.m., $d_{R3} = 3.5$ c.m., $d_{R4} = 3.0$ c.m.			
Tx Dia (c.m.)	6.5	12.5	14.5	15.5	6.5	12.5	14.5	15.5	6.5	12.5	14.5	15.5	6.5	12.5	14.5	15.5
1.0	0.95	0.68	0.57	0.36	0.94	0.68	0.55	0.35	1.51	0.68	0.56	0.36	0.85	0.68	0.47	0.26
2.0	0.93	0.68	0.57	0.35	0.92	0.68	0.55	0.34	1.30	0.68	0.56	0.36	0.83	0.68	0.47	0.25
3.0	0.90	0.66	0.53	0.33	0.90	0.66	0.53	0.31	1.00	0.67	0.54	0.32	0.80	0.67	0.43	0.23
4.0	0.86	0.65	0.50	0.30	0.84	0.65	0.51	0.29	0.95	0.65	0.51	0.30	0.76	0.65	0.40	0.20
5.0	0.81	0.64	0.48	0.28	0.82	0.64	0.47	0.26	0.92	0.64	0.48	0.27	0.71	0.63	0.38	0.18
7.0	0.74	0.61	0.45	0.25	0.73	0.60	0.43	0.22	0.84	0.61	0.45	0.24	0.64	0.61	0.36	0.16
9.0	0.68	0.59	0.42	0.21	0.64	0.59	0.40	0.19	0.76	0.59	0.43	0.21	0.58	0.59	0.34	0.13
10.0	0.58	0.57	0.40	0.20	0.59	0.56	0.37	0.17	0.69	0.57	0.41	0.19	0.48	0.56	0.31	0.11

### 3.5. Overall System Design and Parameter Estimation

The design procedure of the dynamic multiple Rx system by considering the frequency splitting, cross-coupling issues with selective uniform power transfer is illustrated in Figure 9. From the above analysis, the complete system parameter estimation of the proposed method with the selected operating frequency of 1.0 MHz, 1.5 MHz, 2.0 MHz, 3 MHz along with the circuit parameters are presented in Table 3, and different scenarios are considered for the calculation. In scenario 1 the Rx and Tx coils are considered at a fixed distance of 3.5 c.m. and in scenario 2 the distance between Tx and the Rx1, Rx2 and Rx 3, Rx4 are maintained at 3 c.m., 5.5 c.m. respectively.



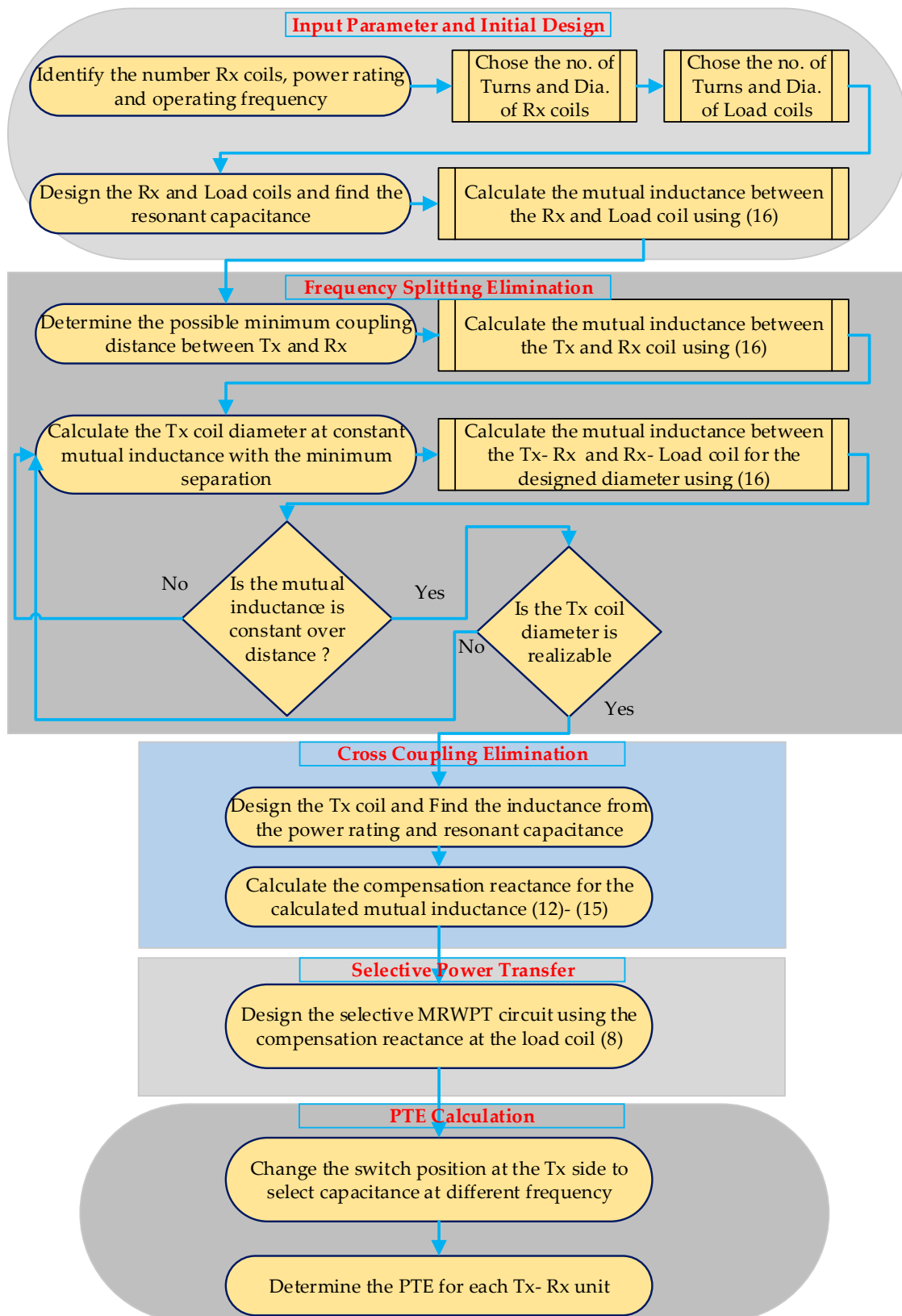


Figure 9. Design Flowchart of Proposed Method.

In scenario 3 and 4 the Rx's positions are changed to 3.5 c.m, 3 c.m, 5.5 c.m, 6.0 c.m and 4 c.m, 3.5 c.m, 4.5 c.m, 7 c.m respectively. In all the cases it is observed the variation in the compensation

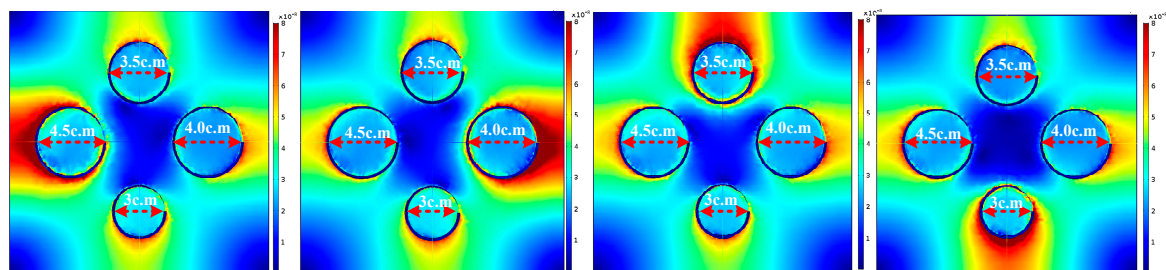
capacitance at the load side is about 0.02 pF to 0.12 pF which can be achieved by using a discrete capacitor at each load coils. Similarly, for the Tx coil diameter of 12.5 c.m, the mutual inductance variation in all the scenarios are from 0.6 to 0.51 which will not deviate the operating frequency of the circuit.

**Table 3.** Calculated Compensation Capacitance for different Scenarios.

Different Scenarios	Tx Coil Diameter (c.m)	Mutual Inductance				Compensating Capacitance at Tx (pF)				Compensating Capacitance at Load (pF)			
		$M_{TR1}$	$M_{TR2}$	$M_{TR3}$	$M_{TR4}$	$f_1$	$f_2$	$f_3$	$f_4$	$C_{Lp1}$	$C_{Lp2}$	$C_{Lp3}$	$C_{Lp4}$
Scenario 1	12.5	0.68	0.68	0.68	0.68	20.2	9.13	5.72	2.21	6.71	8.42	11.23	14.11
Scenario 2	12.5	0.63	0.63	0.55	0.55	20.2	9.13	5.72	2.21	6.42	8.13	10.45	13.91
Scenario 3	12.5	0.68	0.64	0.55	0.54	20.2	9.13	5.72	2.21	6.71	8.22	10.45	13.84
Scenario 4	12.5	0.61	0.66	0.59	0.51	20.2	9.13	5.72	2.21	6.32	8.36	11.11	13.31

#### 4. Finite Element Method Verification

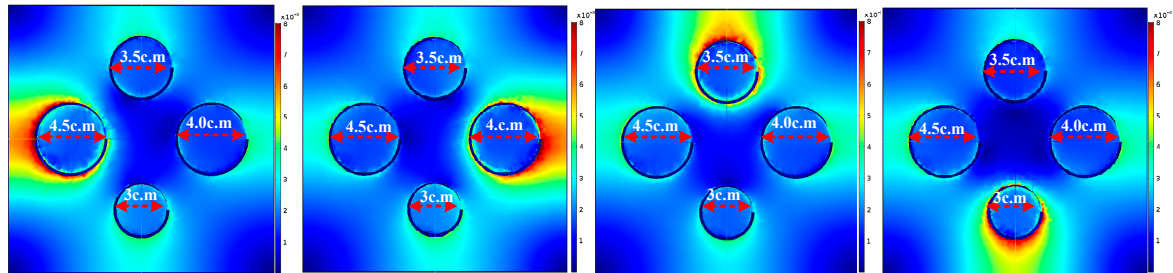
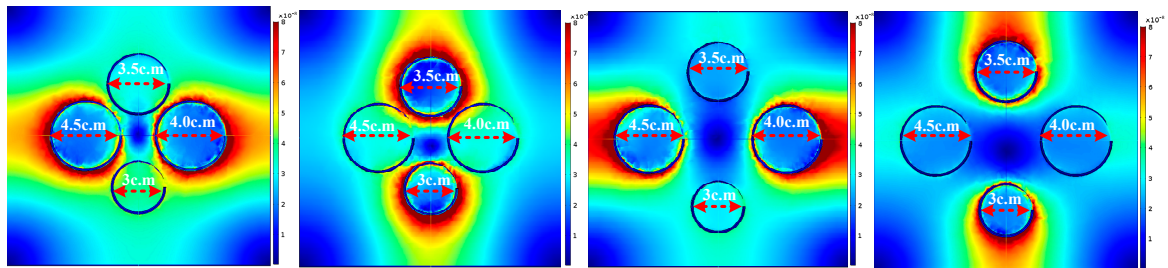
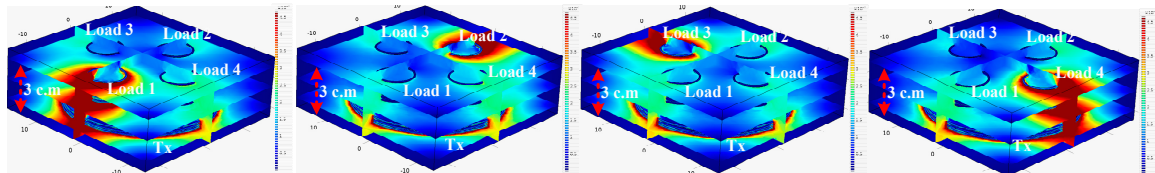
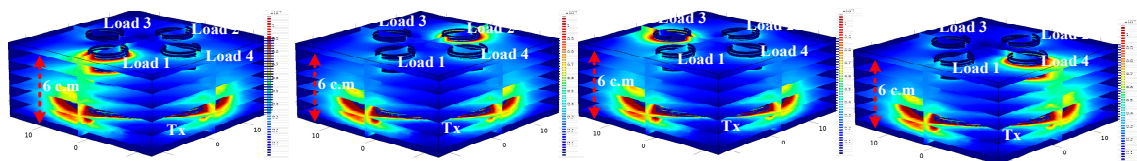
The Finite element modeling of the proposed system is performed using COMSOL Multiphysics software (5.2a, COMSOL Multiphysics Pvt. Ltd., Bengaluru, India) for five different scenarios. The AC/DC module, magnetic field, electric circuit and frequency domain study toolboxes are used to determine the magnetic field intensity on the Rx coils. The physics controlled mesh is used to reduce the computation time and memory usage during the analysis. The coil parameters of the designed system are given in Table 4. The Tx coil is excited with 10 V AC source with selective frequency sweep of 1 MHz, 1.5 MHz, 2 MHz and 3 MHz. First, all the Rx's are considered to be static, and the Tx frequency is switched to match the resonant frequency of each Rx without any cross-coupling compensation. The induced magnetic field on each Rx is shown in Figure 10. It is visible that the selected resonant coil is receiving the maximum field intensity. However, the non-resonant coils magnetic field strength also receiving 40% field strength of resonant coil. In the second case, the compensated capacitor is added to each load coil, and the Tx frequency is switched from 1 MHz, 1.5 MHz, 2 MHz, and 3 MHz to select Rx1 to Rx4 as shown in Figure 11. The magnetic field intensity of the non-resonant coils is less than 15% of the resonant coil, which indicates uniform power distribution to selected load with much reduction of cross coupling. In the third case, the Rx1, Rx2 and Rx3, Rx4 resonant frequency and the corresponding load coil resonant frequency are changed to 1 MHz and 2 MHz respectively. The analysis is performed for two set of the axial distance between the Rx coils as shown in Figure 12. When the distance between the Rx's are reduced to 3 c.m the field strength at non-selected load coil is close to 18% of the resonant coil field strength and when the distance between the Rx coil is increased to 6 c.m the field strength of the non-resonant coil is less than 15%. Finally, the lateral distance between the Tx and Rx, load coils are changed to 3 c.m, 6 c.m and the resonant frequency is switched from 1 MHz to 3 MHz, and the field strength is shown in Figures 13 and 14. In both, the cases the non-resonant coil field is minimum and the resonant coil field is maximum, which indicates the rejection of cross-coupling between the coil and elimination of frequency splitting under over coupled region. The high field strength at the resonant coil indicates the maximum and uniform power delivery to the selected load coil.



**Figure 10.** Magnetic field Intensity of Selective Power Transfer without compensation.

**Table 4.** Design parameters of coil.

Parameters	Tx	Rx1/Load1	Rx2/Load2	Rx3/Load3	Rx4/Load4
Diameter (c.m)	12.5	4.5/4.5	4/4	3.5/3.5	3/3
Number of turns	08	10	8	8	6
Compensation capacitance (pF)	-	6.71	8.42	11.23	14.11
Wire AWG	30	30	30	30	30

**Figure 11.** Magnetic field Intensity of Selective Power Transfer with compensation.**Figure 12.** Magnetic field intensity of two identical frequency Rx with compensation.**Figure 13.** Magnetic field Intensity of Selective Power Transfer with lateral separation of 3 cm.**Figure 14.** Magnetic field Intensity of Selective Power Transfer with lateral separation of 6 cm.

## 5. Experimental Verification

To validate the proposed multiple Rx coil WPT system, an experimental measurement is performed under the static, dynamic environments and the experimental setup is presented in Figure 15. The Tx, Rx and load coils are designed using 30 AWG Litz wire to minimize the ohmic drop in the coil. National Instruments (NI) virtual bench (VB-8012) (National Instruments, Bengaluru, India) is used to give the trigger signal to the power amplifier, and NI myRIO is used for the switching between different capacitive elements to select the different resonant frequency at the Tx coils. Two channel



KEYSIGHT digital storage oscilloscope is used for the measurement of the voltage across each load coils. The dimensions and circuit parameters of the coils are same as the simulation parameters as given in Table 4. Measurements are performed for three different cases as follows.

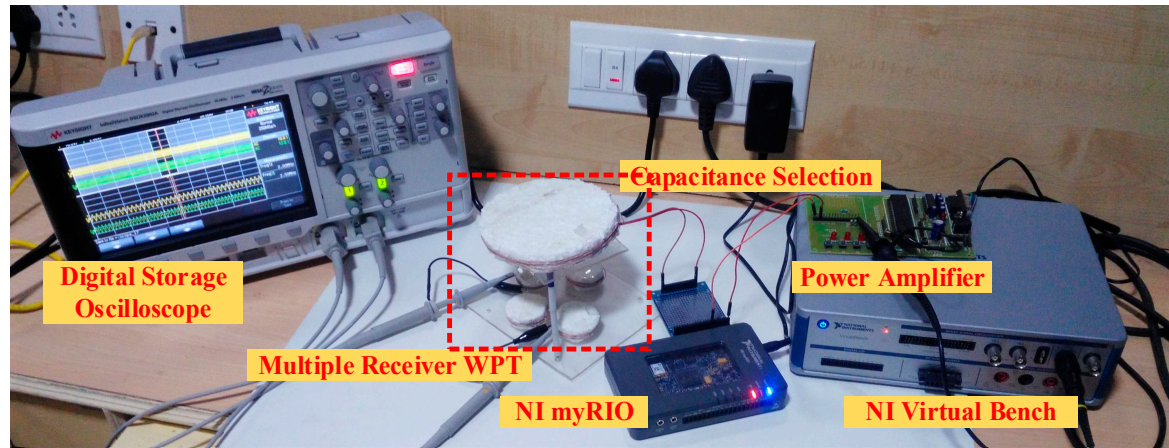


Figure 15. Experimental setup of proposed MRWPT system.

### 5.1. Selective Power Transfer at Static Load Condition

Initially, the separation of the Tx coil and the receiving section is maintained at 5 c.m, and the source and Tx resonant frequency are changed from 1 MHz to 3 MHz to select the Rx 1 to Rx 4. The load coil voltages are measured as shown in Figure 16. Figure 16a represents load-1 and load-2 voltage waveform, when the Tx coil is operated at 1 MHz the voltage at load-1 is 4.8 V and the other load voltages are less than 0.4 V.

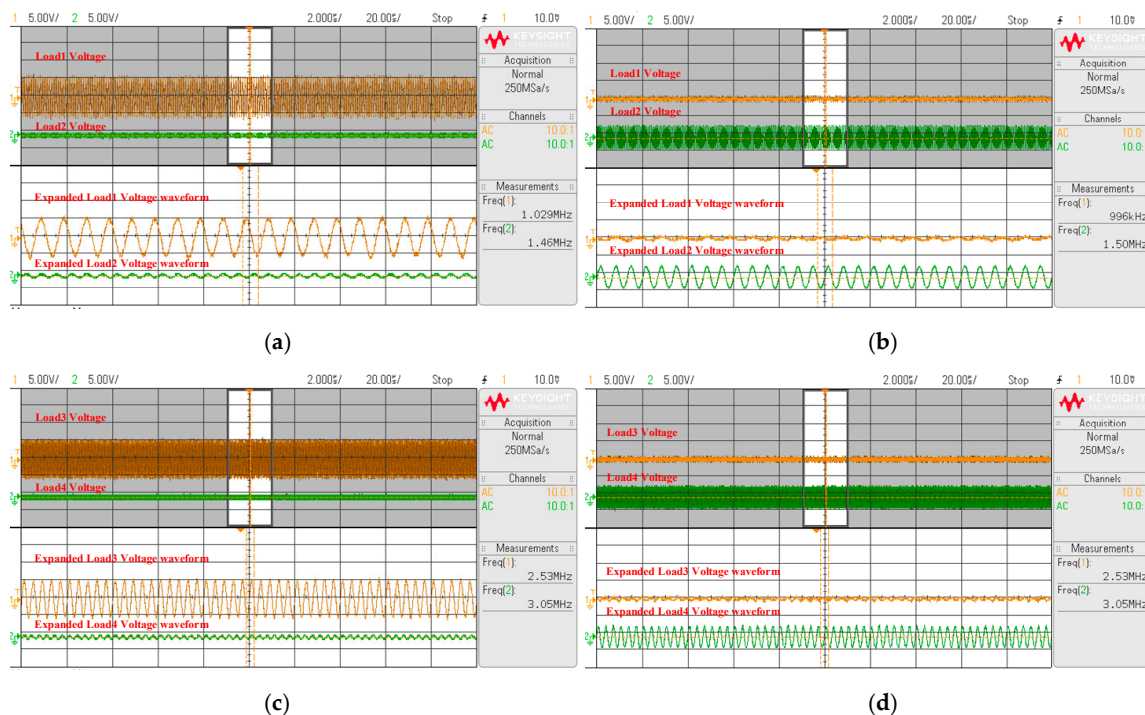
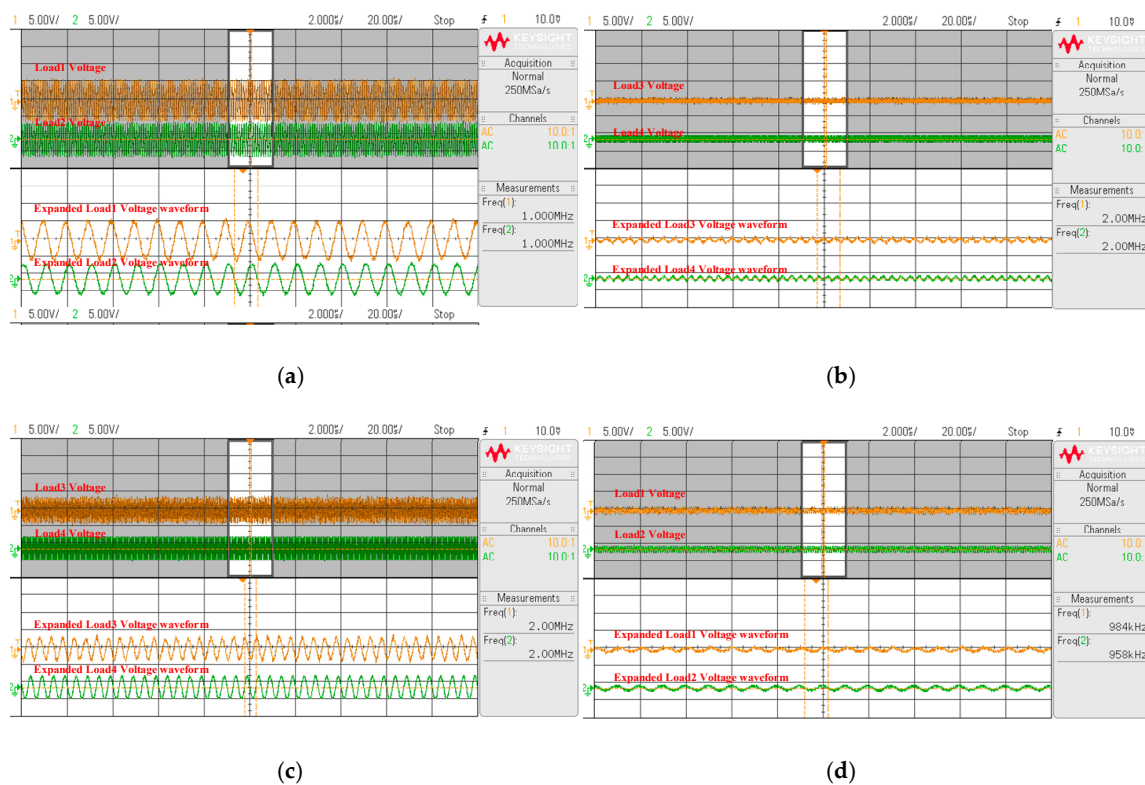


Figure 16. Measured load voltage of selective WPT system. (a)  $f = 1 \text{ MHz}$ ; (b)  $f = 1.5 \text{ MHz}$ ; (c)  $f = 2 \text{ MHz}$ ; (d)  $f = 3 \text{ MHz}$ .

Similarly, when the Tx frequency is changed from 1 MHz to 1.5 MHz, 2 MHz and 3 MHz the respective load coil voltage is increased to more than 4.5 V and other non-resonant load coil voltages are below 0.5 V as shown in Figure 16b–d. It shows that the selective uniform power transfer is accomplished with the very minimal amount of cross coupling. Under the static condition, the effect of frequency splitting also not present in the load voltages as the measured voltage consists of the only single frequency component.

### 5.2. Identical Resonant Frequency Receivers

To analyze the effects of identical frequency the Rx1, Rx2 and Rx3, Rx4 are designed with the resonant frequency of 1 MHz and 2 MHz respectively. Initially, all the distance between the Tx and Rx are maintained at 5 c.m, and the operating frequency of the Tx is selected at 1.0 MHz. The load-1 and load-2 voltages are maximum at 1 MHz operating condition and load-3, load-4 voltages are less than 0.5 V as shown in Figure 17a,b. Next, the operating frequency is changed to 2 MHz the load-3 and load-4 voltages are at 4.6 V, 4.4 V respectively and the load-1, load-2 voltages are less than 0.4 V as shown in Figure 17c,d respectively. It is observed that the effect of cross coupling on each Rx is reduced and both the coil voltages are reached more than 4.4 V under the identical resonant frequency condition. The uniform power distribution to the selected Rx also obtained as the non-resonant coil voltages are less than 0.4 V.



**Figure 17.** Measured load voltage of selective wireless power transfer (WPT) with two identical Rx resonant frequency (a)  $V_{L1}$ ,  $V_{L2}$  at  $f_{r1} = f_{r2} = 1$  MHz (b)  $V_{L3}$ ,  $V_{L4}$  at  $f_{r1} = f_{r2} = 1$  MHz (c)  $V_{L3}$ ,  $V_{L4}$  at  $f_{r3} = f_{r4} = 2$  MHz (d)  $V_{L1}$ ,  $V_{L2}$  at  $f_{r3} = f_{r4} = 2$  MHz.

### 5.3. Dynamic Conditions

The Rx1 position is changed to analyze the effects of dynamic conditions, the Rx2, Rx3 and Rx4 positions are kept constant. The induced voltage at load-1 varying from 6.4 V to 4.2 V for the variation of separation from 3 c.m to 7 c.m as shown in Figure 18a,b at 1 MHz. The load-2, load-3 and load-4 are designed with the resonant frequency of 1.5 MHz, 2 MHz, 3 MHz respectively. The non-resonant

load voltages are less than 0.45 V as shown in Figure 18a,b. The effect of cross coupling on each Rx is reduced, and the frequency splitting also eliminated for the closer coupling distance of 3 c.m. The measured frequency of the load-1 voltage at 3 c.m is of 1 MHz, and the frequency deviation is not present in the load-1.

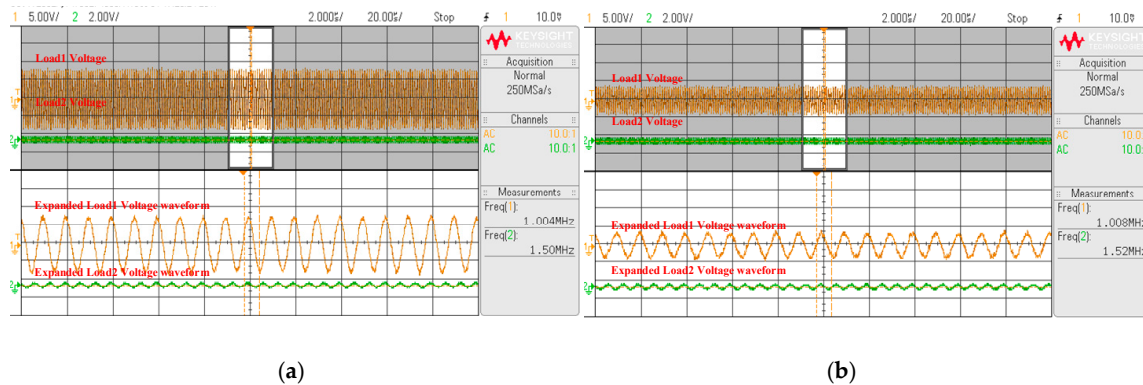


**Figure 18.** Measured load voltage of selective WPT system with load-1 variation (a) Rx1 at 3 c.m; (b) Rx1 at 7 c.m.

The comparative analysis of the proposed method with the existing design in the literature is presented in Table 5. It is observed that the proposed design for the Rx WPT system with identical or non-identical operating frequency gives a better and simple solution to eliminate frequency splitting and cross coupling with improved PTE.

**Table 5.** Comparison of Proposed Method with Literature for Multiple Receiver WPT.

Methods of Reference	No. of Tx	No. of Rx	No. of Relay	$f$ (MHz)	Remarks
Multiple Rx, Multiple Tx [15]	2	2	0	1 MHz	Requires two Tx and analyzed under static condition
Selective Power Transfer [24]	1	3	0	21.5 MHz to 23.5 MHz	Suitable for uniform power transfer and cross-coupling issue for identical Rx's
Cross-Coupling Elimination [27]	1	3	0	1 MHz	The uniform power distribution and frequency splitting elimination is not achieved
Dynamic Rx WPT [20]	1	3	0	1 MHz	The cross-coupling and frequency splitting is not addressed
This Work	1	4	1	1 MHz to 3 MHz	The cross-coupling, frequency splitting issue is addressed with selective power transfer

## 6. Conclusions

The analysis and design of WPT to multiple Rx system is discussed in this paper by considering the cross-coupling, frequency splitting, and uniform power distribution challenges. The simulation, finite element analysis on the four Rx WPT system for different scenarios of static and dynamic Rx's are performed. To minimize the effects of cross-coupling, the capacitive compensation to the individual load coil is investigated and from the analysis it is observed that the capacitive compensation provides the less electromagnetic interference. It can be suitable for tiny electronics or medical implants where the device size is the major constraints. Further, to improve the uniform power distribution to the selected Rx a three-coil based selective MRWPT system is accomplished by tuning the Tx frequency to match the Rx resonant frequency. The simulation and the experimental results show that the proposed design technique could be the simple and better solution for the multiple Rx WPT system.



**Author Contributions:** All authors contributed equally to the research work and its final decimation as article in its current form.

**Conflicts of Interest:** The authors declare no conflict of interest.

## References

1. Jiang, C.; Chau, K.T.; Liu, C.; Lee, C.H.T. An Overview of Resonant Circuits for Wireless Power Transfer. *Energies* **2017**, *10*, 894. [[CrossRef](#)]
2. Kim, J.G.; Wei, G.; Kim, M.H.; Jong, J.Y.; Zhu, C. A Comprehensive Study on Composite Resonant Circuit-based Wireless Power Transfer Systems. *IEEE Trans. Ind. Electron.* **2017**, *PP*, 1. [[CrossRef](#)]
3. Jawad, A.M.; Nordin, R.; Gharghan, S.K.; Jawad, H.M.; Ismail, M. Opportunities, and Challenges for Near-Field Wireless Power Transfer: A Review. *Energies* **2017**, *10*, 1022. [[CrossRef](#)]
4. Huang, C.; Kawajiri, T.; Ishikuro, H. A 13.56-MHz Wireless Power Transfer System with Enhanced Load-Transient Response and Efficiency by Fully Integrated Wireless Constant-Idle-Time Control for Biomedical Implants. *IEEE J. Solid-State Circuits* **2017**, *PP*, 1–14. [[CrossRef](#)]
5. Narayanamoorthi, R.; Juliet, A.V.; Chokkalingam, B.; Padmanaban, S.; Leonowicz, Z.M. Class E Power Amplifier Design and Optimization for the Capacitive Coupled Wireless Power Transfer System in Biomedical Implants. *Energies* **2017**, *10*, 1409. [[CrossRef](#)]
6. Dinis, H.; Colmiais, I.; Mendes, P.M. Extending the Limits of Wireless Power Transfer to Miniaturized Implantable Electronic Devices. *Micromachines* **2017**, *8*, 359. [[CrossRef](#)]
7. Agarwal, K.; Jegadeesan, R.; Guo, Y.X.; Thakor, N.V. Wireless Power Transfer Strategies for Implantable Bioelectronics. *IEEE Rev. Biomed. Eng.* **2017**, *10*, 136–161. [[CrossRef](#)] [[PubMed](#)]
8. Lu, Y.; Ma, D.B. Wireless Power Transfer System Architectures for Portable or Implantable Applications. *Energies* **2016**, *9*, 1087. [[CrossRef](#)]
9. Ahn, D.; Mercier, P.P. Wireless Power Transfer with Concurrent 200-kHz and 6.78-MHz Operation in a Single-Transmitter Device. *IEEE Trans. Power Electron.* **2016**, *31*, 5018–5029. [[CrossRef](#)]
10. Huang, S.; Li, Z.; Lu, K. Frequency splitting suppression method for four-coil wireless power transfer system. *IET Power Electron.* **2016**, *9*, 2859–2864. [[CrossRef](#)]
11. Zhang, Y.; Zhao, Z.; Chen, K. Frequency-Splitting Analysis of Four-Coil Resonant Wireless Power Transfer. *IEEE Trans. Ind. Appl.* **2014**, *50*, 2436–2445. [[CrossRef](#)]
12. Huang, R.; Zhang, B.; Qiu, D.; Zhang, Y. Frequency Splitting Phenomena of Magnetic Resonant Coupling Wireless Power Transfer. *IEEE Trans. Magn.* **2014**, *50*, 8600204. [[CrossRef](#)]
13. Fu, M.; Yin, H.; Ma, C. Megahertz Multiple-Receiver Wireless Power Transfer Systems with Power Flow Management and Maximum Efficiency Point Tracking. *IEEE Trans. Microw. Theory Tech.* **2017**, *65*, 4285–4293. [[CrossRef](#)]
14. Tan, L.; Guo, J.; Huang, X.; Wen, F. Output power stabilisation of wireless power transfer system with multiple transmitters. *IET Power Electron.* **2016**, *9*, 1374–1380. [[CrossRef](#)]
15. Johari, R.; JKrogmeier, V.; Love, D.J. Analysis and Practical Considerations in Implementing Multiple Transmitters for Wireless Power Transfer via Coupled Magnetic Resonance. *IEEE Trans. Ind. Electron.* **2014**, *61*, 1774–1783. [[CrossRef](#)]
16. Monti, G.; Dionigi, M.; Mongiardo, M.; Perfetti, R. Optimal Design of Wireless Energy Transfer to Multiple Receivers: Power Maximization. *IEEE Trans. Microw. Theory Tech.* **2017**, *65*, 260–269. [[CrossRef](#)]
17. Tang, S.C.; Lun, T.L.T.; Guo, Z.; Kwok, K.W.; McDannold, N.J. Intermediate Range Wireless Power Transfer with Segmented Coil Transmitters for Implantable Heart Pumps. *IEEE Trans. Power Electron.* **2017**, *32*, 3844–3857. [[CrossRef](#)]
18. Liu, X.; Wang, G. A Novel Wireless Power Transfer System with Double Intermediate Resonant Coils. *IEEE Trans. Ind. Electron.* **2016**, *63*, 2174–2180. [[CrossRef](#)]
19. Huang, X.; Gao, Y.; Zhou, J.; Ma, J.; Zhang, J.; Fang, Y. Magnetic field design for optimal wireless power transfer to multiple receivers. *IET Power Electron.* **2016**, *9*, 1885–1893. [[CrossRef](#)]
20. Lee, K.; Cho, D.H. Diversity Analysis of Multiple Transmitters in Wireless Power Transfer System. *IEEE Trans. Magn.* **2013**, *49*, 2946–2952. [[CrossRef](#)]
21. Ng, W.M.; Zhang, C.; Lin, D.; Hui, S.R. Two- and Three-Dimensional Omnidirectional Wireless Power Transfer. *IEEE Trans. Power Electron.* **2014**, *29*, 4470–4474. [[CrossRef](#)]

22. Chabalko, M.J.; Sample, A.P. Three-Dimensional Charging via Multimode Resonant Cavity Enabled Wireless Power Transfer. *IEEE Trans. Power Electron.* **2015**, *30*, 6163–6173. [[CrossRef](#)]
23. Fu, M.; Zhang, T.; Ma, C.; Zhu, X. Efficiency and Optimal Loads Analysis for Multiple-Receiver Wireless Power Transfer Systems. *IEEE Trans. Microw. Theory Tech.* **2015**, *63*, 801–812. [[CrossRef](#)]
24. Kim, Y.J.; Ha, D.; Chappell, W.J.; Irazoqui, P.P. Selective Wireless Power Transfer for Smart Power Distribution in a Miniature-Sized Multiple-Receiver System. *IEEE Trans. Ind. Electron.* **2016**, *63*, 1853–1862. [[CrossRef](#)]
25. Cui, D.; Imura, T.; Hori, Y. Cross coupling cancellation for all frequencies in multiple-receiver wireless power transfer systems. In Proceedings of the 2016 International Symposium on Antennas and Propagation (ISAP), Okinawa, Japan, 24–28 October 2016; pp. 48–49.
26. Lee, G.; Waters, B.H.; Mahoney, B.J.; Smith, J.R.; Park, W.S. An investigation of cross-coupling for magnetically coupled wireless power transfer. In Proceedings of the 2013 Asia-Pacific Microwave Conference Proceedings (APMC), Seoul, Korea, 5–8 November 2013; pp. 80–82.
27. Fu, M.; Zhang, T.; Zhu, X.; Luk, P.C.K.; Ma, C. Compensation of Cross Coupling in Multiple-Receiver Wireless Power Transfer Systems. *IEEE Trans. Ind. Inform.* **2016**, *12*, 474–482. [[CrossRef](#)]
28. Li, Y.; Mai, R.; Lu, L.; Lin, T.; Liu, Y.; He, Z. Analysis and Transmitter Currents Decomposition Based Control for Multiple Overlapped Transmitters Based WPT Systems Considering Cross Couplings. *IEEE Trans. Power Electron.* **2018**, *33*, 1829–1842. [[CrossRef](#)]
29. Du, S.; Chan, E.; Wen, B.; Hong, J.; Widmer, H.; Wheatley, C. Wireless Power Transfer Using Oscillating Magnets. *IEEE Trans. Ind. Electron.* **2017**, *PP*, 1. [[CrossRef](#)]
30. Niu, W.; Gu, W.; Chu, J.; Shen, A. Frequency splitting patterns in wireless power relay transfer. *IET Circuits Devices Syst.* **2014**, *8*, 561–567. [[CrossRef](#)]
31. Seo, D.W.; Lee, J.H. Frequency-Tuning Method Using the Reflection Coefficient in a Wireless Power Transfer System. *IEEE Microw. Wirel. Compon. Lett.* **2017**, *27*, 959–961. [[CrossRef](#)]
32. Lyu, Y.L.; Meng, F.Y.; Yang, G.H.; Che, B.J.; Wu, Q.; Sun, L.; Erni, D.; Li, J.L.W. A Method of Using Nonidentical Resonant Coils for Frequency Splitting Elimination in Wireless Power Transfer. *IEEE Trans. Power Electron.* **2015**, *30*, 6097–6107. [[CrossRef](#)]
33. Cha, H.K.; Park, W.T.; Je, M. A CMOS Rectifier With a Cross-Coupled Latched Comparator for Wireless Power Transfer in Biomedical Applications. *IEEE Trans. Circuits Syst. II* **2012**, *59*, 409–413. [[CrossRef](#)]
34. Kang, S.H.; Choi, J.H.; Jung, C.W. Magnetic resonance wireless power transfer using three-coil system with single planar receiver for laptop applications. *IEEE Trans. Consum. Electron.* **2015**, *61*, 160–166. [[CrossRef](#)]
35. Porto, R.W.; Brusamarello, V.J.; Müller, I.; Riaño, F.L.C.; De Sousa, F.R. Wireless power transfer for contactless instrumentation and measurement. *IEEE Instrum. Meas. Mag.* **2017**, *20*, 49–54. [[CrossRef](#)]



© 2018 by the authors. Licensee MDPI, Basel, Switzerland. This article is an open access article distributed under the terms and conditions of the Creative Commons Attribution (CC BY) license (<http://creativecommons.org/licenses/by/4.0/>).